Climate
of the Past

Open Access

EGU

Supplement of

Multiple thermal Atlantic Meridional Overturning Circulation thresholds in the intermediate complexity model Bern3D

Markus Adloff et al.

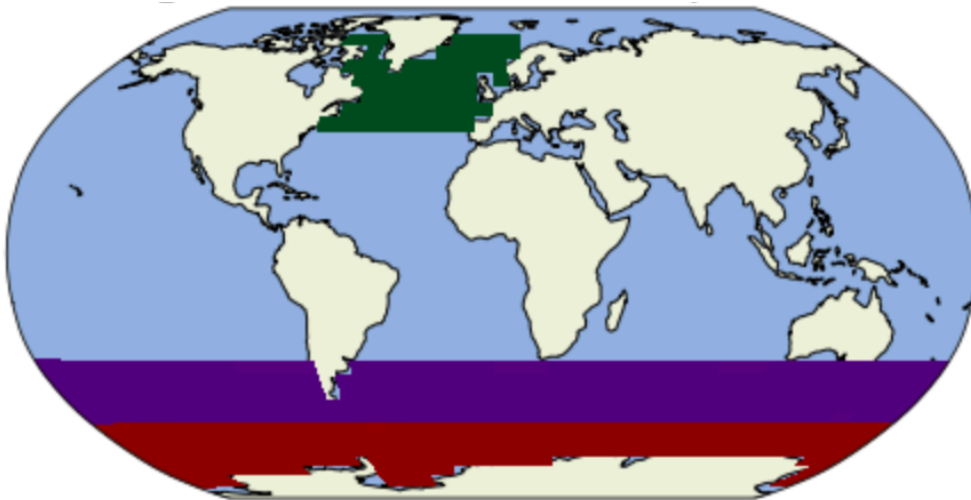*Correspondence to:* Markus Adloff (markus.adloff@unibe.ch)

Figure S1: Locations of different circulation tracer surface restoration: Green - NADW, Purple - AAIW, Red - AABW.
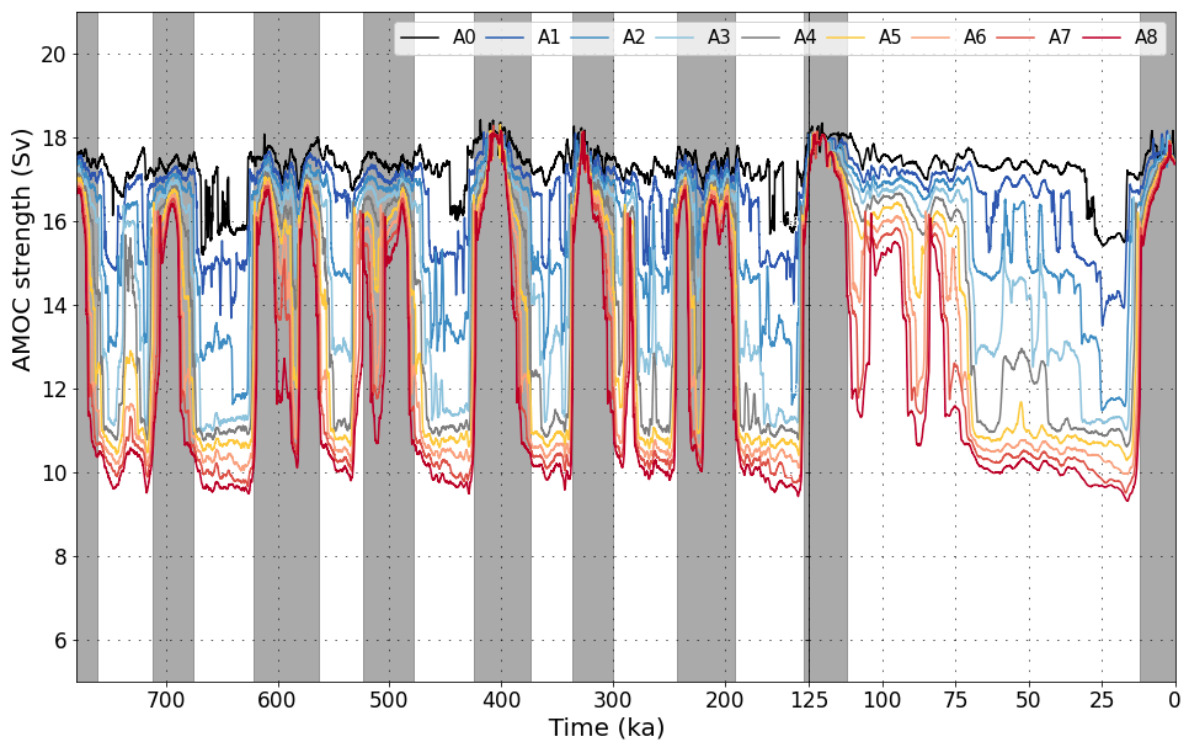

Figure S2: Maximum AMOC strength over the last eight glacial cycles as simulated in simulation set A. Gray intervals indicate interglacials.
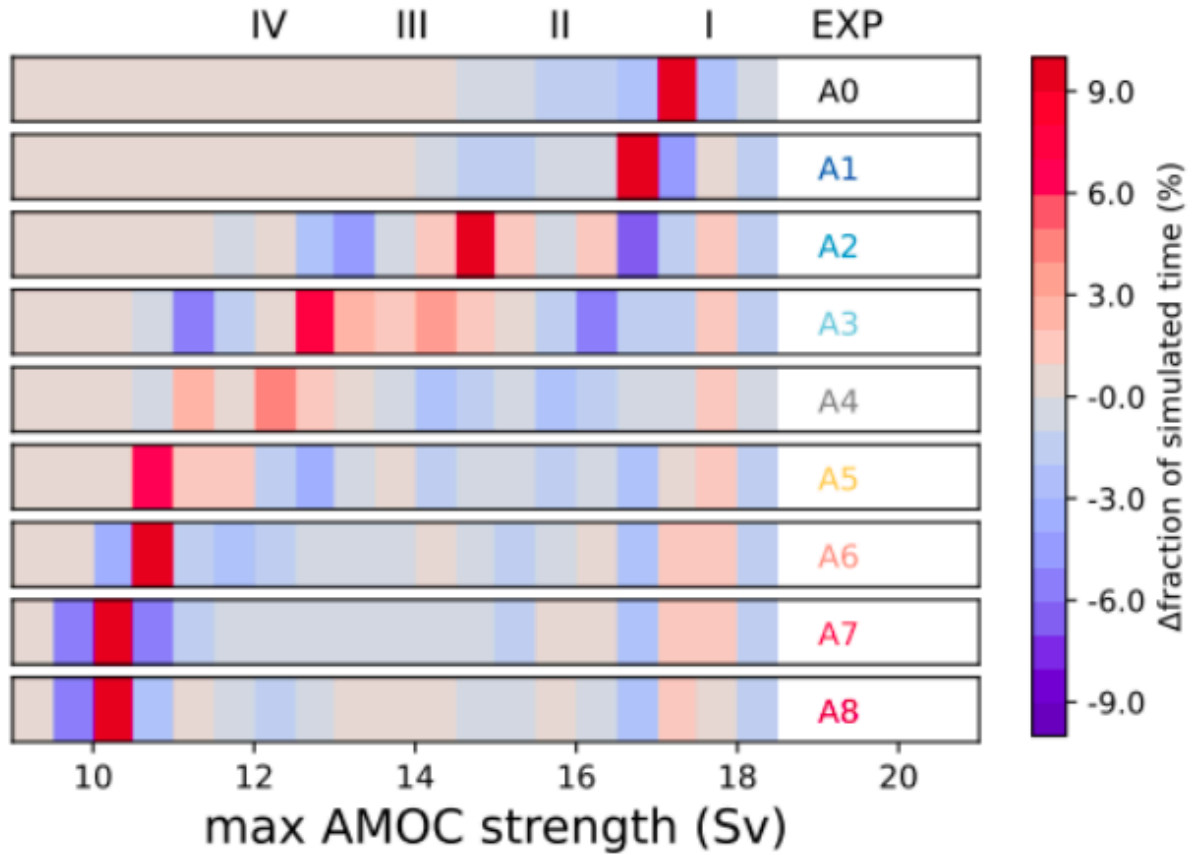
Figure S2: Similar to Fig 2, but showing the difference of AMOC strength occurrence before and after the Mid-Brunhes transition (positive values = more frequent occurrence after the transition). Each row shows the results of one simulation, the simulation ID is given on the right end of the column in colours that correspond to the lines in Fig 1. The bins are 0.5 Sv wide.
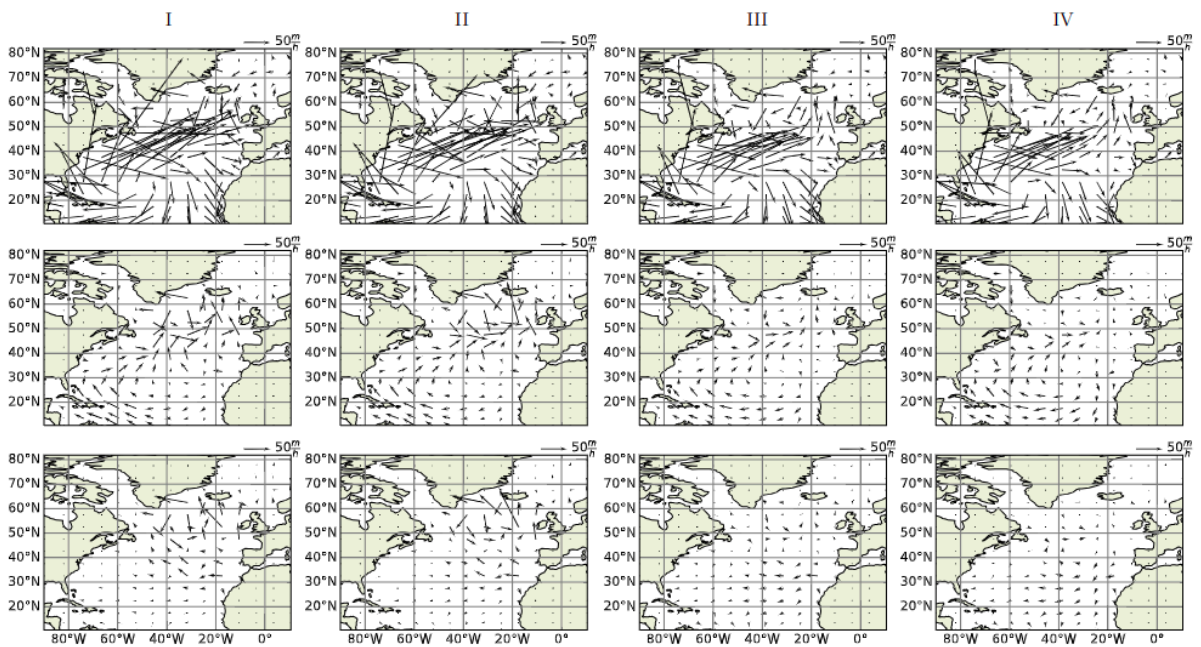
Figure SI.3: Vector plots of ocean velocities in three different depths (upper row: 100m, middle row: 600m, lower row: 1000m) in the North Atlantic in each circulation state defined by AMOC strength.
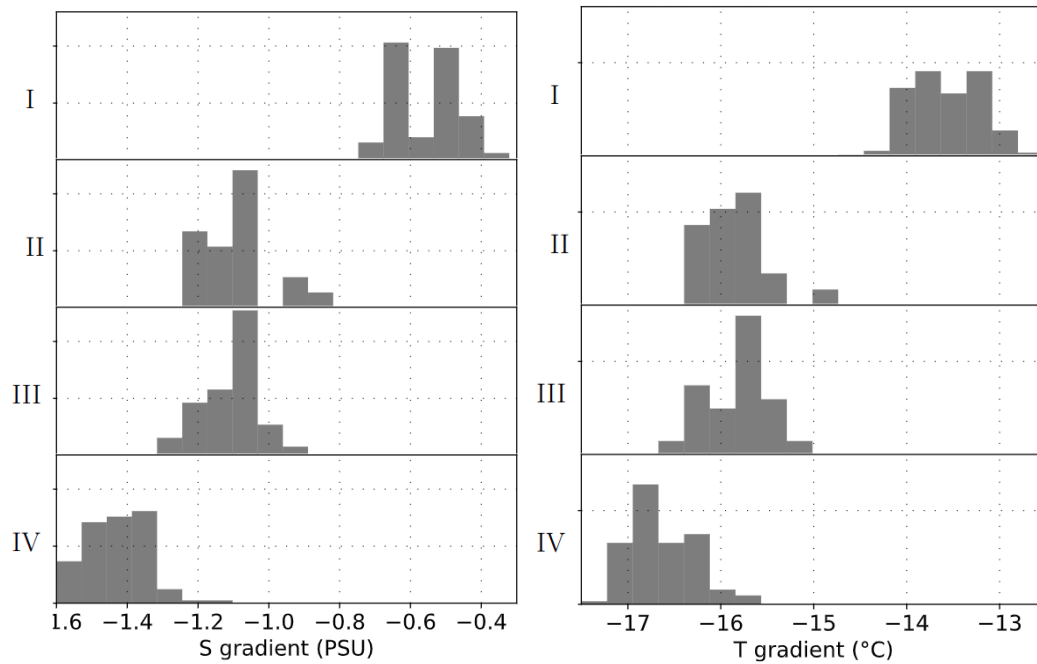

Figure S4: Occurrence of salinity and temperature differences between the Irminger and the Caribbean seas in all time slices that fall into one of the four states defined by their AMOC strength in simulation A3.
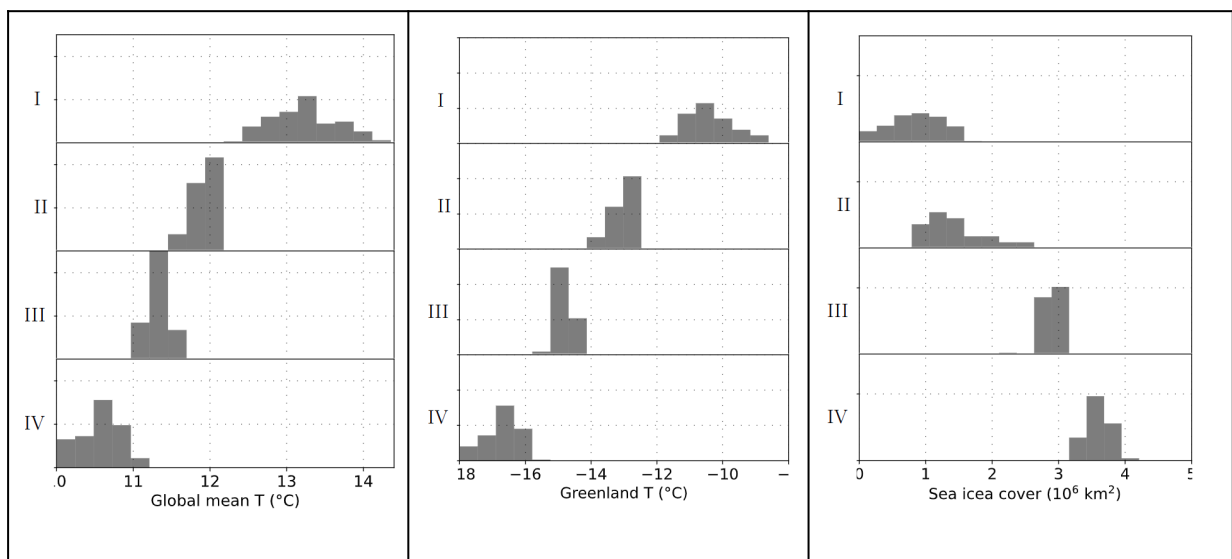

Figure S5: Occurrence of Global mean temperature, Greenland temperature and sea ice cover in the North East Atlantic in all time slices that fall into one of the four states defined by their AMOC strength in simulation A3.
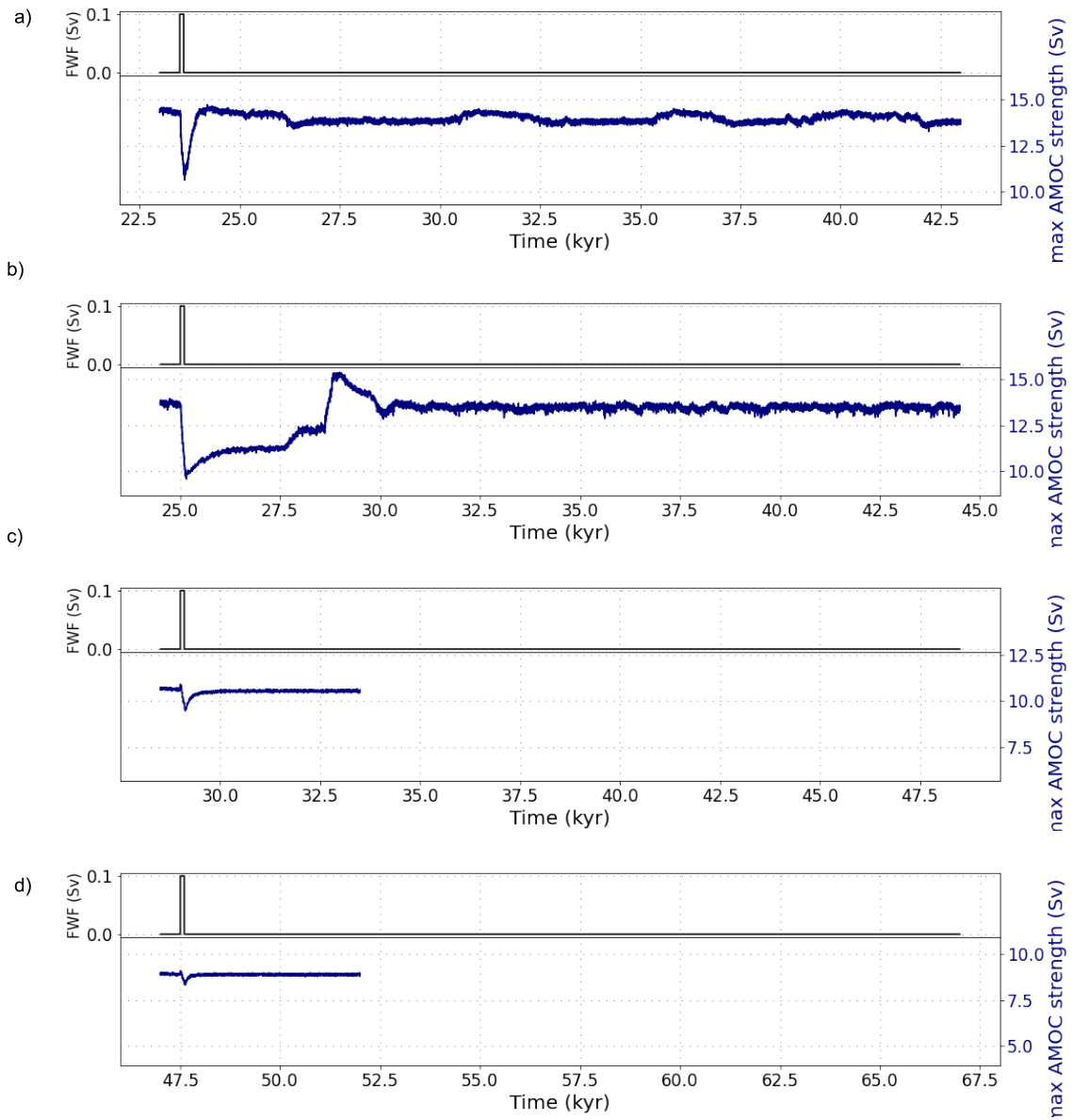
Figure S6: Circulation mode stability tests for four time slices from simulation B.slow: 23 kyr (a), 24.5 kyr (b), 28.5 kyr (c) and 47 kyr (d). FWF = external Freshwater flux
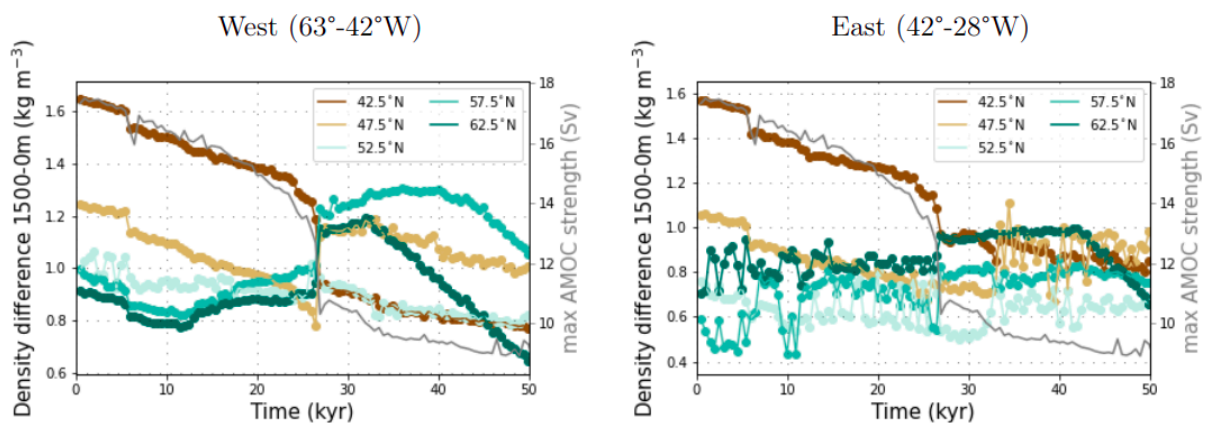
Figure S7: Density differences over the top 1500 m of the water column at different latitudes in the western and eastern North Atlantic over the first 50 kyr of simulation B.slow.
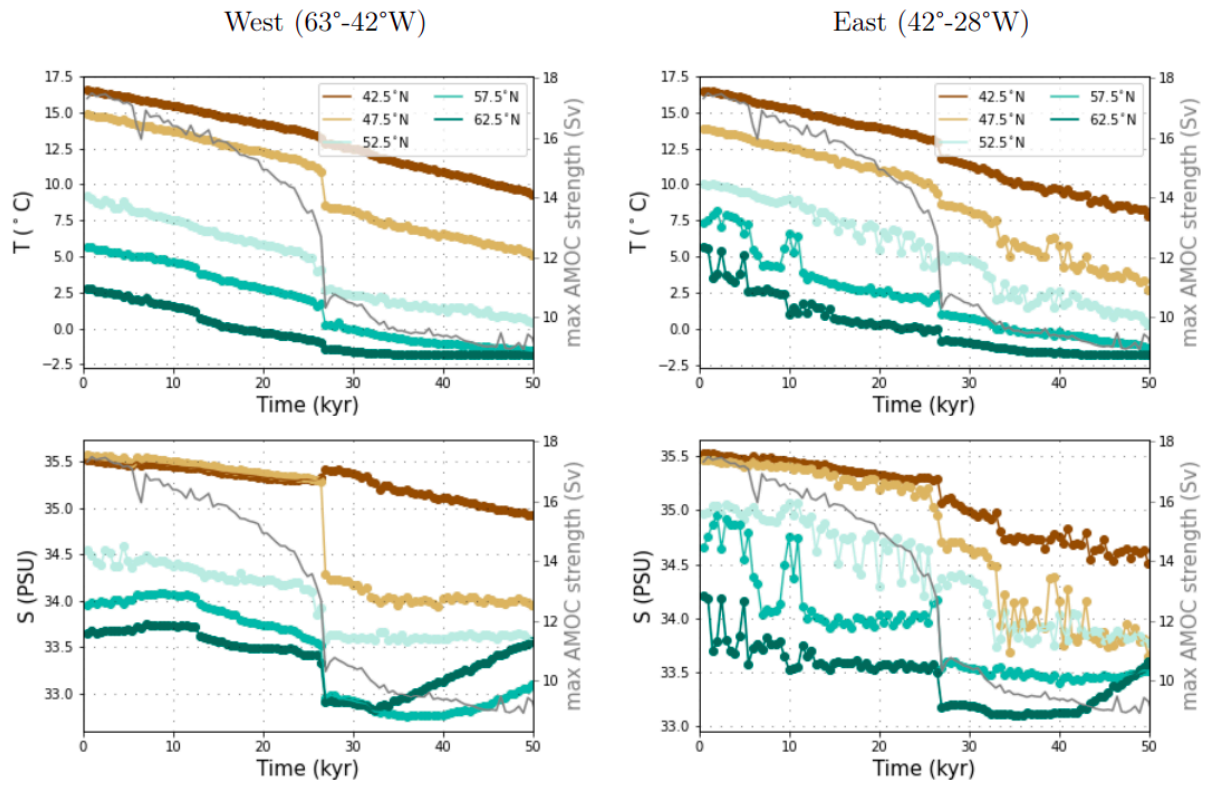

Figure S8: Surface temperature and salinity at different latitudes in the western and eastern North Atlantic over the first 50 kyr of simulation B.slow.
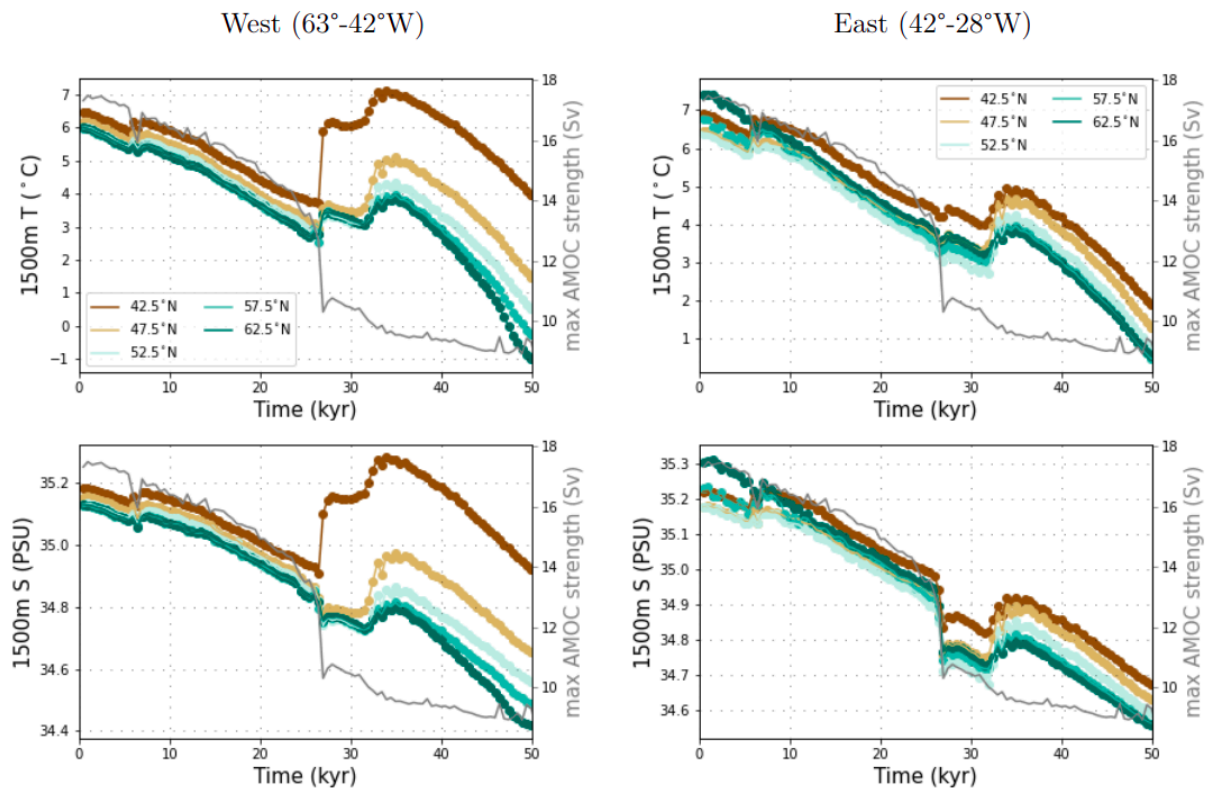
Figure S9: Temperature and salinity at 1500 m depth at different latitudes in the western and eastern North Atlantic over the first 50 kyr of simulation B.slow.
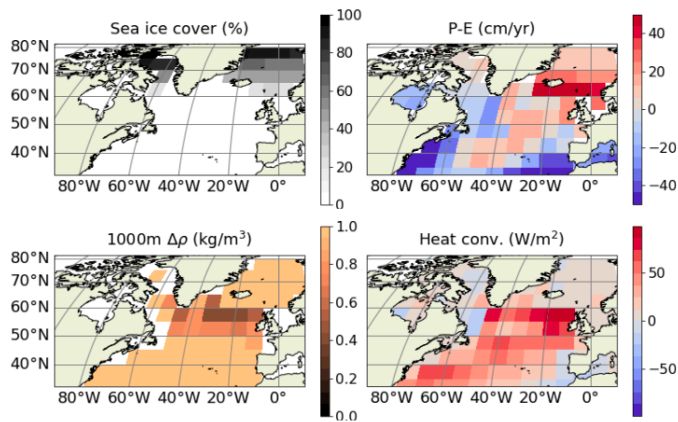

Figure S10: Initial sea ice cover, meteoric freshwater balance, heat convergence in the ocean, and the density difference over the upper 1000 m of the water column in the North Atlantic at the beginning of simulation B.slow.
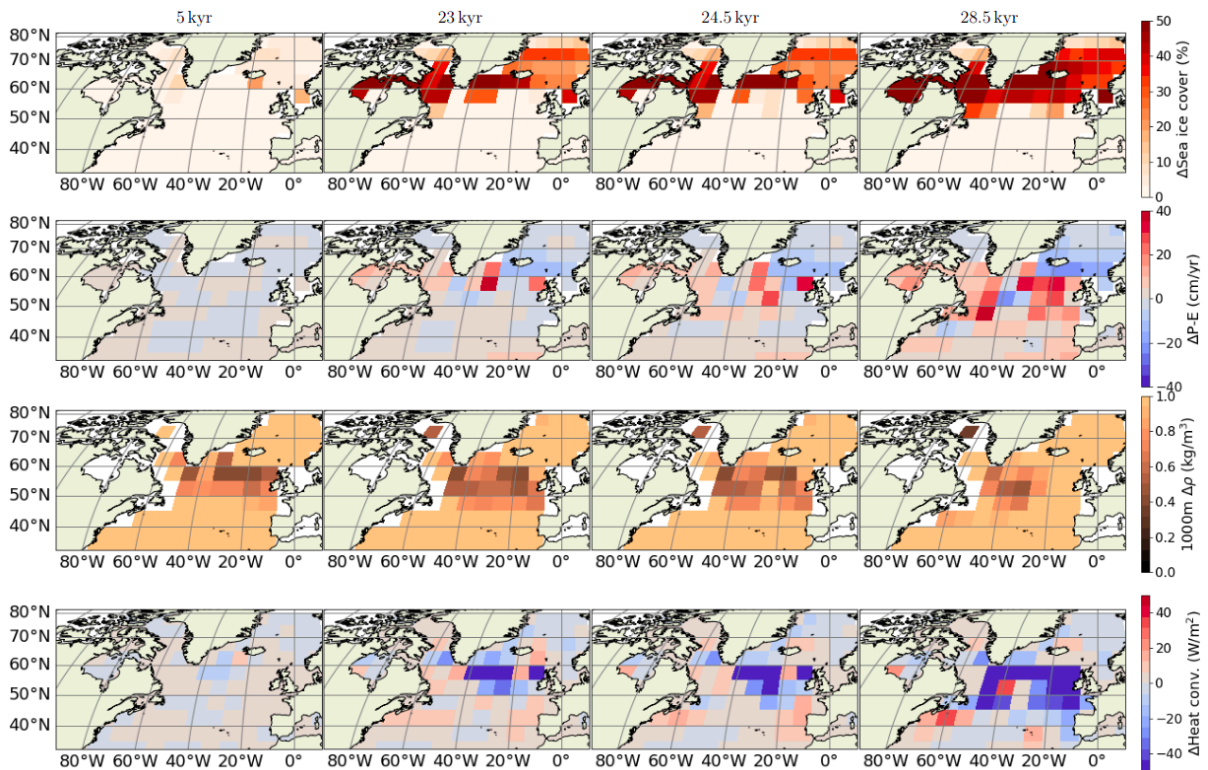
Figure S11: Changes in Sea ice cover, meteoric freshwater balance and heat convergence in the ocean, and the density difference over the upper 1000 m of the water column in the North Atlantic over the first 30 kyr of simulation B.slow. The initial states of the four variables are shown in Fig. S10
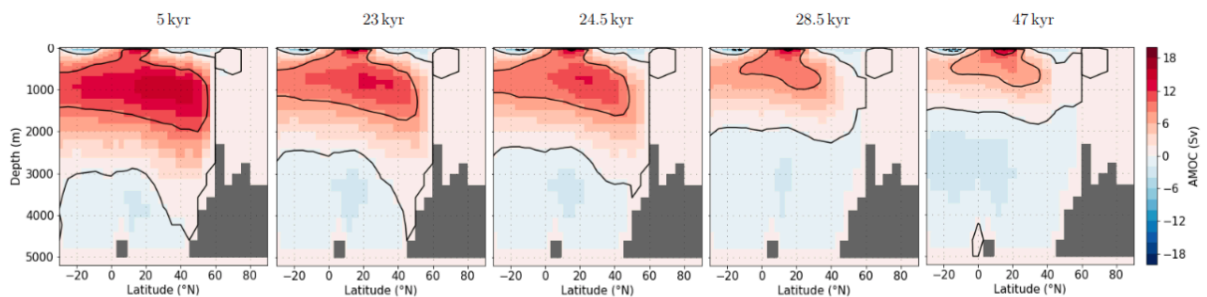

Figure S12: AMOC streamfunction at different time slices of simulation B.slow
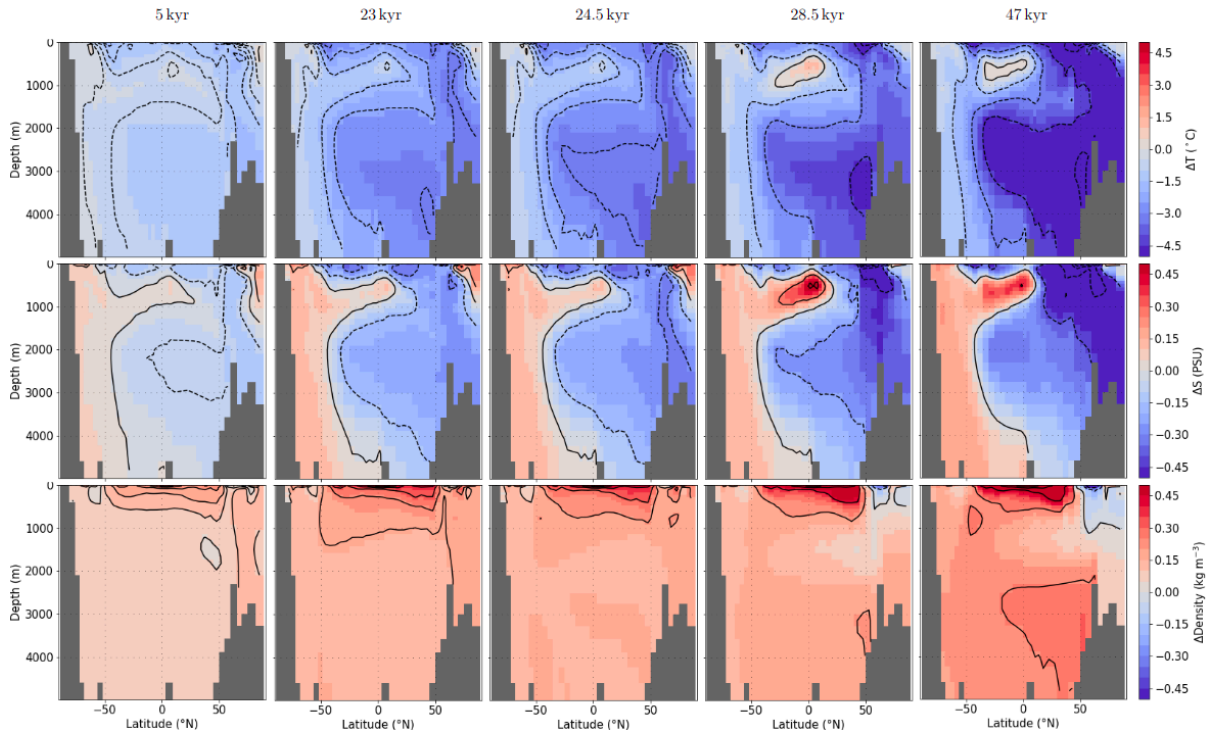
Figure S13: Atlantic zonal means of temperature, salinity, and density anomalies (relative to the start of the simulation at different time slices of simulation B.slow.
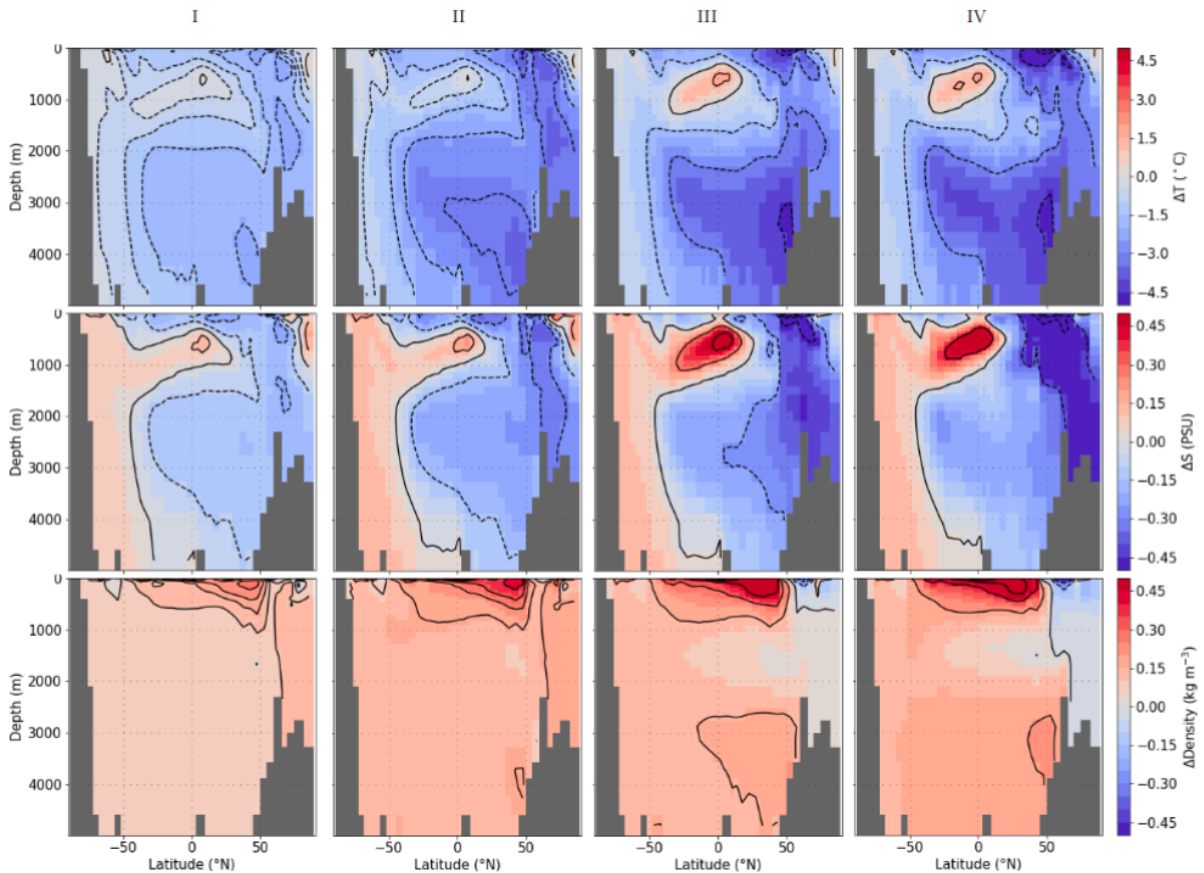

Figure S14: Atlantic zonal means of temperature, salinity, and density changes (relative to pre-industrial) in the Atlantic basin for the four circulation states adopted across the last glacial cycle in simulation A3.
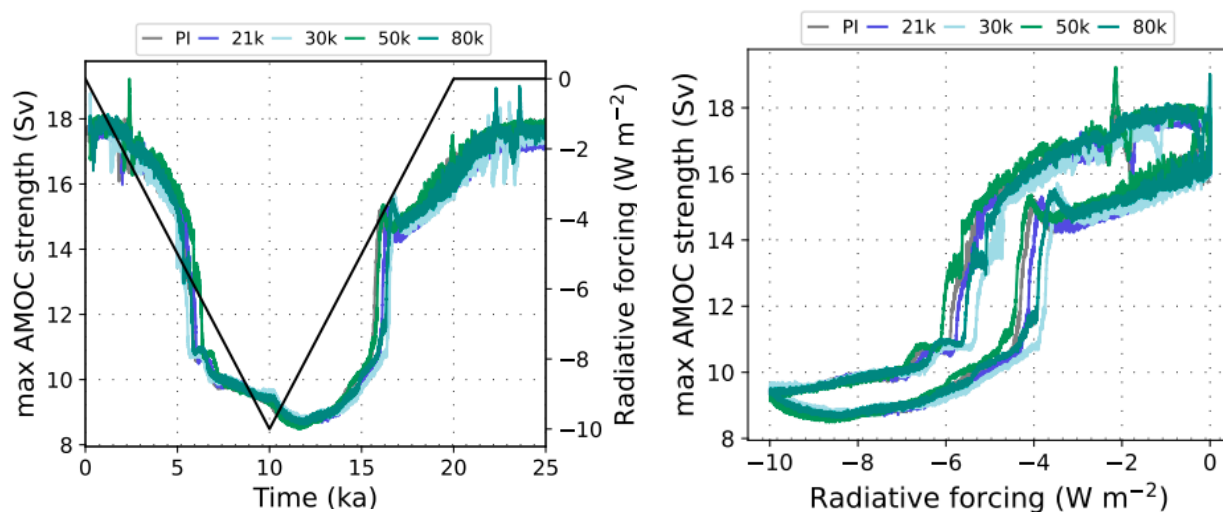
Figure S15: Response of the AMOC strength to changes in radiative forcing and hysteresis behaviour under different orbital configurations in simulations B.fast.PI, B.fast.21k, B.fast.30k, B.fast.50k, B.fast.80.

Simulation	Eccentricity	Obliquity (°)	Precession	65°N July Insolation (W/m^2)
B.fast.PI	0.01724	23.446	0.017	426.76
B.fast.21k	0.01940	22.989	0.018	418.62
B.fast.30k	0.01690	22.255	-0.009	438.63
B.fast.50k	0.01493	24.416	0.011	449.88
B.fast.80k	0.02884	23.175	-0.021	463.07

Table S1: Orbital parameters for the B.fast simulation set.